

¹³C–²⁷Al TRAPDOR and REDOR Experiments for the Detection of ¹³C–²⁷Al Dipolar Interactions in Solids

Leo van Wüllen¹ and Martin Kalwei

Institut für Physikalische Chemie, Westfälische Wilhelms-Universität Münster, Schlossplatz 4-7, D-48149 Münster, Germany

Received September 9, 1998; revised March 17, 1999

We report ¹³C–²⁷Al double resonance experiments (REDOR and TRAPDOR) on several aluminum organic compounds with the aim of detecting ¹³C–²⁷Al dipolar couplings and distances in solids. The ¹³C and ²⁷Al pulses are applied to the same probe channel because their resonance frequencies are in close proximity. The different possibilities of controlling the efficiency of the TRAPDOR approach (by varying the ²⁷Al RF amplitude and the MAS frequency) are investigated. The results indicate that TRAPDOR is superior to REDOR in resolving differences in ¹³C–²⁷Al distances when choosing the proper experimental conditions. Where known, the crystal structure data are in qualitative agreement with the distance information extracted from our experiments. The experiment should be very valuable in different fields of solid state chemistry, where the interaction of organic and inorganic sample fractions is of fundamental importance. © 1999 Academic Press

INTRODUCTION

The measurement of internuclear distances and connectivities in high resolution solid state nuclear magnetic resonance has become one of the most powerful tools for the structural characterization in a wide variety of materials. Double resonance techniques such as transfer of populations in double resonance (TRAPDOR) (1–4), rotational echo double resonance (REDOR) (5–7), and rotational echo adiabatic passage double resonance (REAPDOR) (8, 9) have been successfully employed in the structural characterization of zeolites (10–15), glasses (16, 17), and catalysts (18). Hardware requirements limit the application of these methods to *I* and *S* nuclei, whose resonance frequencies differ by at least 10 MHz. Thus, the study of heteronuclear dipolar interactions among nuclei whose resonance frequencies lie within the above-mentioned range (for example, ²³Na–⁵¹V, ²³Na–²⁷Al, ¹³C–²⁷Al) seems to be excluded. Especially the combination ¹³C–²⁷Al attracts much attention because of its predominant importance in studying host/guest interactions in catalytically relevant systems. In a recent paper we introduced a modified TRAPDOR experiment to detect dipolar couplings between these two nuclei (19). The experiment, in which the pulses for the ¹³C and ²⁷Al frequen-

cies are applied to the same probe channel, was successful in resolving differences in the three different ¹³C–²⁷Al distances in the chosen model compound, aluminum lactate.

In the present paper we examine the opportunities of controlling the magnitude of the TRAPDOR effect (i.e., maximizing the TRAPDOR difference signal and sensitivity) and compare the results with those obtained using modified REDOR spectroscopy. Since the TRAPDOR efficiency depends on the quadrupolar coupling strength of the ²⁷Al nuclei, different model compounds with quadrupolar coupling constants ranging from 3.0 to 8 MHz are studied.

EXPERIMENTAL

The samples, aluminum lactate (Al(lact)₃), aluminum acetylacetonate (Al(acac)₃), and hydroxylaluminum diacetate (Al(Oac)₂OH) were purchased from Aldrich and used without further purification. Aluminum triacetate was synthesized as follows: 9.4 g Al(OEt)₃ (Aldrich) was mixed with 50 ml acetic anhydride and refluxed at 150°C for 5 h. The precipitate was dried *in vacuo* at 100°C.

The TRAPDOR and REDOR NMR experiments were performed on a modified Bruker CXP 200 spectrometer operating at 4.7 T, equipped with a Tecmag MacSpec upgrade. The resonance frequencies were 50.32, 52.15, and 200.13 MHz for ¹³C, ²⁷Al, and ¹H, respectively. The ¹³C and ¹H radiofrequency pulses were provided by the spectrometer console. An external frequency synthesizer (PTS 310) in combination with a Tecmag DecKit IV was used for the generation and control of the ²⁷Al radiofrequency pulses.

The ¹³C and ²⁷Al radiofrequency signals were then fed into a HF switch (Mini-circuits) which could be triggered by the pulse sequence via a TTL signal. With this setup, either the ¹³C pulses (low TTL signal) or the ²⁷Al pulses (high TTL signal) are passed through to the amplification stages and finally into the probe.

A standard Bruker 7 mm CPMAS probe was used in these experiments. Sufficiently short $\pi/2$ pulse lengths on the ¹³C and ²⁷Al frequencies simultaneously were obtained in the following way: The bandwidth of the resonant circuit was increased by

¹ To whom correspondence should be addressed.

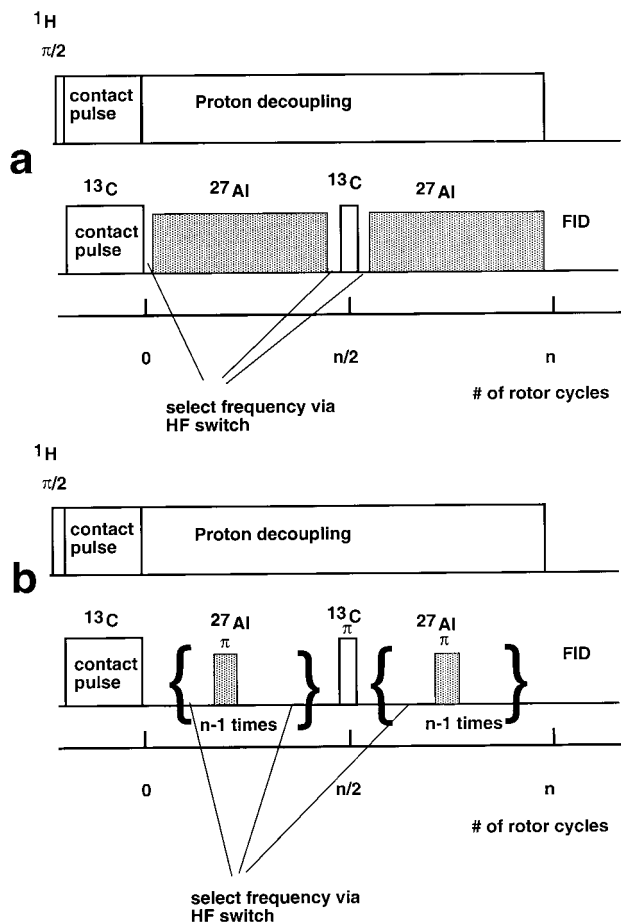


FIG. 1. Pulse sequences used in this work. (a) TRAPDOR; (b) REDOR. The ^{13}C and ^{27}Al pulses are applied to the same probe channel.

placing a resistor parallel to the sample coil and the probe was then tuned to the center frequency between the two resonance frequencies (51.2 MHz). The resulting (liquid) $\pi/2$ pulse lengths were found to be 6 and 9 μs for ^{13}C and ^{27}Al , respectively.

Figure 1 shows the pulse sequences used in this work. In these sequences the X and Y pulses are applied to the one probe X channel. The switching between the ^{13}C (X) and ^{27}Al (Y) frequencies is achieved by selecting one of them via the HF switch. The 5 μs time delay between pulses for the two different frequencies accounts for pulse ringdown and switching time.

The ^{27}Al MAS spectra were recorded at two different B_0 field strengths on a Bruker CXP300 operating at 7.04 T (ν_0 ^{27}Al = 78.17 MHz) and a Bruker DSX 500 spectrometer operating at 11.7 T (ν_0 ^{27}Al = 130.29 MHz) using standard Bruker 4 mm MAS probes and spinning speeds of 14 kHz.

RESULTS

Standard NMR Characterization of the Model Compounds

Aluminum Acetylacetonate

The ^{13}C CPMAS spectrum of aluminum acetylacetonate is shown in Fig. 2a(i). The three carbon signals are assigned to the carbonyl carbon (C_2 : 191.4 ppm), methylene carbon (C_3 : 101.6 ppm), and methyl carbon (C_1 : 27.8 ppm), respectively. The geometrically and electronically very symmetric octahedral environment imparts a rather small quadrupolar coupling constant on the aluminum sites in this sample. This is confirmed by the ^{27}Al MAS spectra depicted in Fig. 2b(i). From a simulation of the central transition MAS spectra (not shown) we obtain a quadrupolar coupling constant of 3.0 MHz and an asymmetry parameter of 0.1 (cf. Table 1).

Aluminum Lactate

Three signals can be identified in the ^{13}C CPMAS spectrum of aluminum lactate (Fig. 2a(ii)) and assigned to the three different carbon atoms in the lactate molecule as follows: The signal at 179 ppm arises from the carboxylate carbons (C_1), the component at 69 ppm originates in the C_2 carbons, and the resonance at 17 ppm is due to the methyl carbons (C_3) of the lactate. The ^{27}Al MAS spectra (Fig. 2b(ii)) exhibit well structured complicated signals. With the help of an additional SATRAS experiment [20, 21] (not shown) we determined a quadrupolar coupling constant of approximately 5 MHz and an asymmetry parameter of 0.5 (Table 1). Simulations of the central transition MAS spectra taken at 7 and 11.7 T with these parameters reproduce the characteristic features of the spectra.

Aluminum Acetates

The ^{27}Al MAS spectra of the hydroxylaluminum diacetate (Fig. 2b(iii)) reveal very broad signals due to a large quadrupolar coupling constant of approximately 8 MHz (estimated from the differences of the center of gravity of the spectra taken at different field strengths). The ^{13}C CPMAS spectrum (Fig. 2a(iii)) exhibits two signals arising from the methyl carbon (at 5.3 ppm) and the carboxylate carbon at 160.9 ppm.

Although aluminum triacetate could not be prepared in pure form, the NMR characterization shows that the resulting compound is suitable for ^{13}C - ^{27}Al double resonance experiments. The ^{13}C CPMAS spectrum of the resulting compound (Fig. 2a(iv)) consists of two resonances at 3.7 and 158.6 ppm. The ^{27}Al MAS spectra (Fig. 2b(iv)) show two features: a narrow resonance centered around 5 ppm with a quadrupolar coupling constant of 2.4 MHz and a broad structured signal centered around -18 ppm. The compound hydrolyzes very quickly, and the broad signal probably arises from these hydrolysis products.

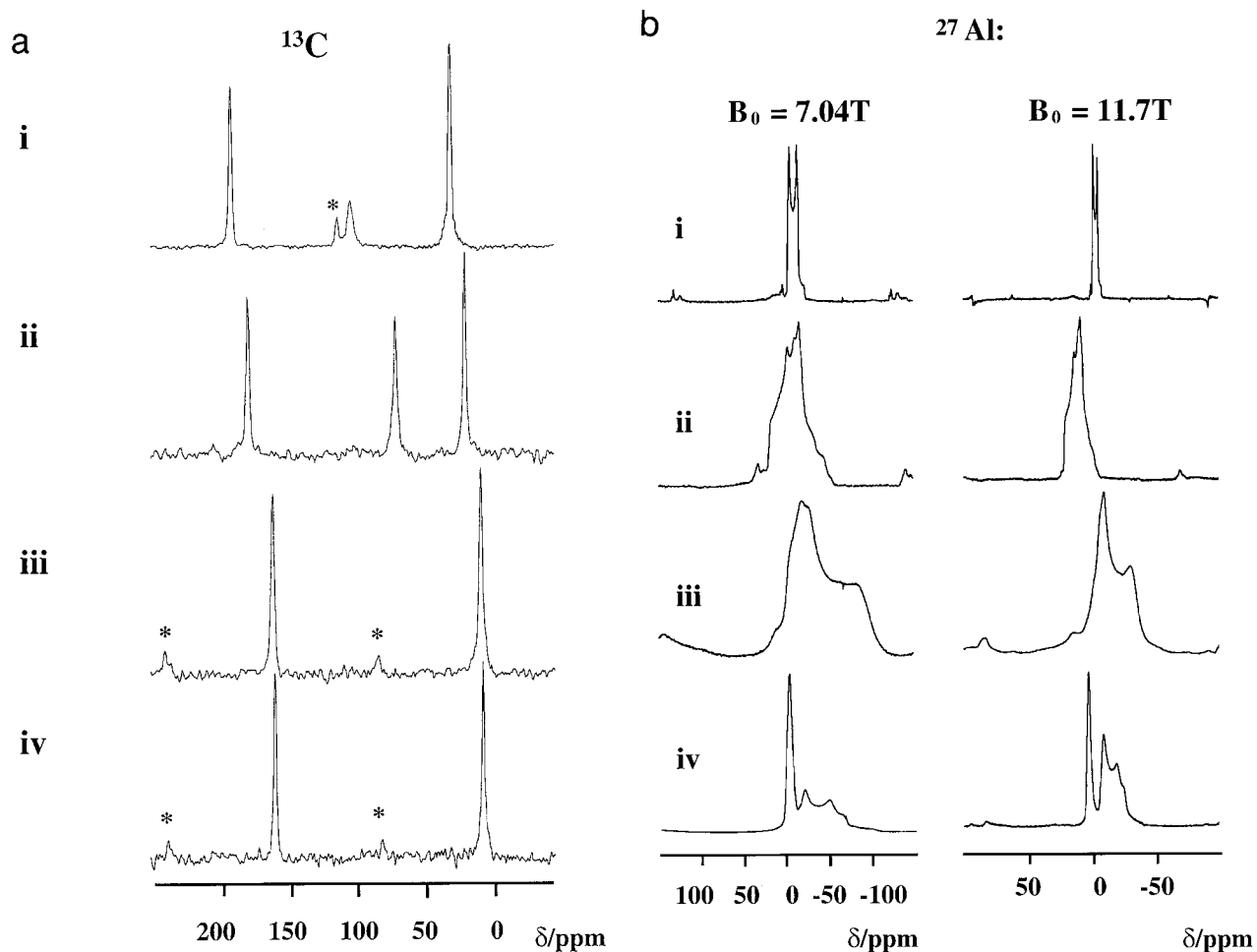
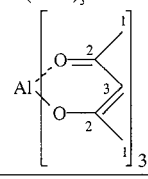
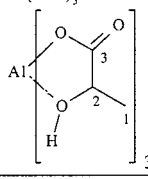


FIG. 2. (a) ^{13}C CPMAS spectra of the samples studied. (b) ^{27}Al MAS spectra at $B_0 = 7.04$ and 11.7 T. Spinning sidebands are indicated by asterisks. (i) $\text{Al}(\text{acac})_3$, (ii) $\text{Al}(\text{lact})_3$, (iii) $\text{Al}(\text{Oac})_2\text{OH}$, and (iv) $\text{Al}(\text{Oac})_3$.

TRAPDOR and REDOR Experiments

Figure 3 shows the results of a TRAPDOR experiment on $\text{Al}(\text{acac})_3$. The top spectrum is the result of a ^{13}C CPMAS spin echo experiment (giving rise to the signal intensities S_0), and the middle spectrum was obtained using the TRAPDOR sequence described in Fig. 1. The relative size of the TRAPDOR effect for the three different carbon sites in $\text{Al}(\text{acac})_3$, expressed as the ratio of the TRAPDOR difference signal to the full echo signal intensity $(S_0 - S)/S_0$ (Fig. 3, bottom) indicate ^{13}C - ^{27}Al dipolar couplings increasing in the order $^{13}\text{C}_1$ - ^{27}Al (methyl carbon), $^{13}\text{C}_3$ - ^{27}Al (methylene carbon), and $^{13}\text{C}_2$ - ^{27}Al (carbonyl carbon). Figure 4 reveals a plot of the TRAPDOR fraction $(S_0 - S)/S_0$ for the individual ^{13}C resonances versus the dipolar evolution time NT_r . In this plot, the initial slope and steepness of the resulting TRAPDOR curves are roughly proportional to the dipolar coupling strengths and hence to the inverse cubes of the closest ^{13}C - ^{27}Al internuclear distances.

TABLE 1
 ^{13}C - ^{27}Al Internuclear Distances, ^{27}Al Quadrupole Parameters and Chemical Shift Values for the Model Compounds $\text{Al}(\text{acac})_3$, $\text{Al}(\text{lact})_3$, $\text{Al}(\text{Oac})_3$, and $\text{Al}(\text{Oac})_2\text{OH}$

Sample	C_Q	η_Q	δ_{iso}	Carbon	Distance
$\text{Al}(\text{acac})_3$: 	3,03 MHz	0,1	-0,3 ppm	1	425 pm
				2	283 pm
				3	325 pm
$\text{Al}(\text{lact})_3$: 	5 MHz	0,5	21,8 ppm	1	390 pm
				2	285 pm
				3	270 pm
$\text{Al}(\text{Oac})_3$	2,4 MHz	-	5 ppm		
$\text{Al}(\text{Oac})_2\text{OH}$	≈ 8 MHz	-	11 ppm		

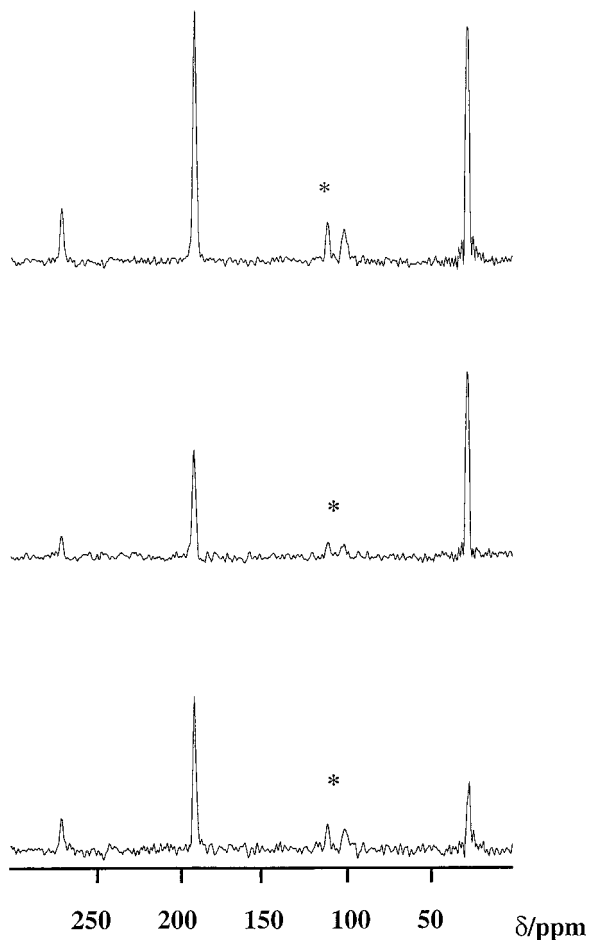


FIG. 3. TRAPDOR spectra of $\text{Al}(\text{acac})_3$ at 40 rotor cycles; $\nu_{\text{MAS}} = 4$ kHz. $\pi/2(^{13}\text{C}) = 6.5$ μs , $\nu_{\text{RF}}(^{27}\text{Al}) = 22$ kHz. Top spectrum: ^{13}C CPMAS spin echo; middle spectrum: ^{13}C - ^{27}Al TRAPDOR; bottom spectrum: TRAPDOR difference. Spinning sidebands are indicated by asterisks.

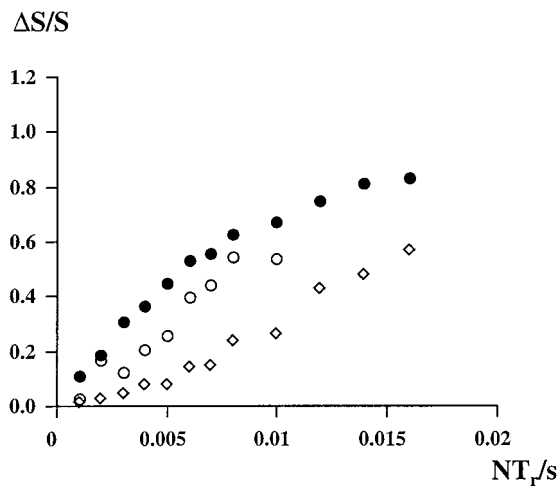


FIG. 4. Plot $\Delta S/S_0$ versus dipolar evolution time for $\text{Al}(\text{acac})_3$; $\nu_{\text{MAS}} = 4$ kHz. $\pi/2(^{13}\text{C}) = 6.5$ μs , $\nu_{\text{RF}}(^{27}\text{Al}) = 22$ kHz. Filled circles, C_2 (carbonyl carbon); open circles, C_3 (methylene carbon); open diamonds, C_1 (methyl carbon).

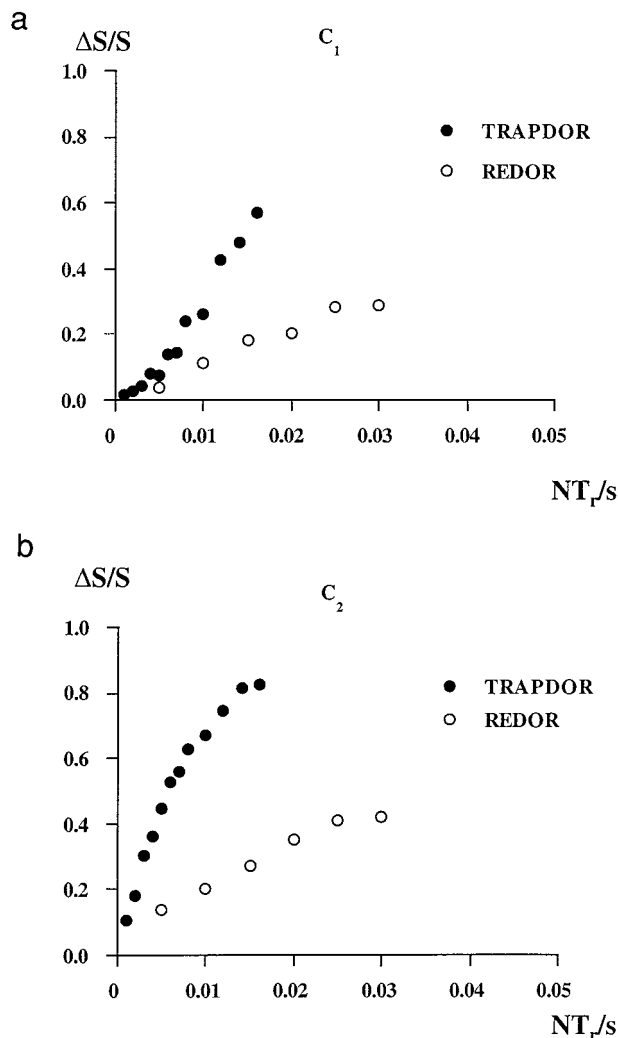


FIG. 5. Comparison of REDOR and TRAPDOR. (a) Methyl resonance. (b) Carbonyl resonance of $\text{Al}(\text{acac})_3$. Experimental details: REDOR: $\nu_{\text{MAS}} = 4$ kHz, $\pi/2(^{13}\text{C}) = 5.0$ μs , $\nu_{\text{RF}}(^{27}\text{Al}) = 20$ kHz; TRAPDOR: $\nu_{\text{MAS}} = 4$ kHz, $\pi/2(^{13}\text{C}) = 6.5$ μs , $\nu_{\text{RF}}(^{27}\text{Al}) = 22$ kHz.

Figs. 5a and b compare the resulting TRAPDOR curves with those obtained by the REDOR approach for the methyl carbons (Fig. 5a) and carbonyl carbons (Fig. 5b) in $\text{Al}(\text{acac})_3$. It is clear from inspection of this figure that the REDOR approach is much less sensitive in detecting ^{13}C - ^{27}Al dipolar couplings than the TRAPDOR approach.

Figure 6 illustrates the influence of the MAS frequency on the magnitude of the TRAPDOR effect. Shown are the TRAPDOR curves for the carbonyl carbon (Fig. 6a) and methyl carbon (Fig. 6b) of $\text{Al}(\text{acac})_3$ obtained for rotational frequencies of 1, 2, and 4 kHz using the pulse sequence described in Fig. 1a and varying the number of rotor cycles. In both cases the initial slope and steepness of the TRAPDOR curves and hence the magnitude of the

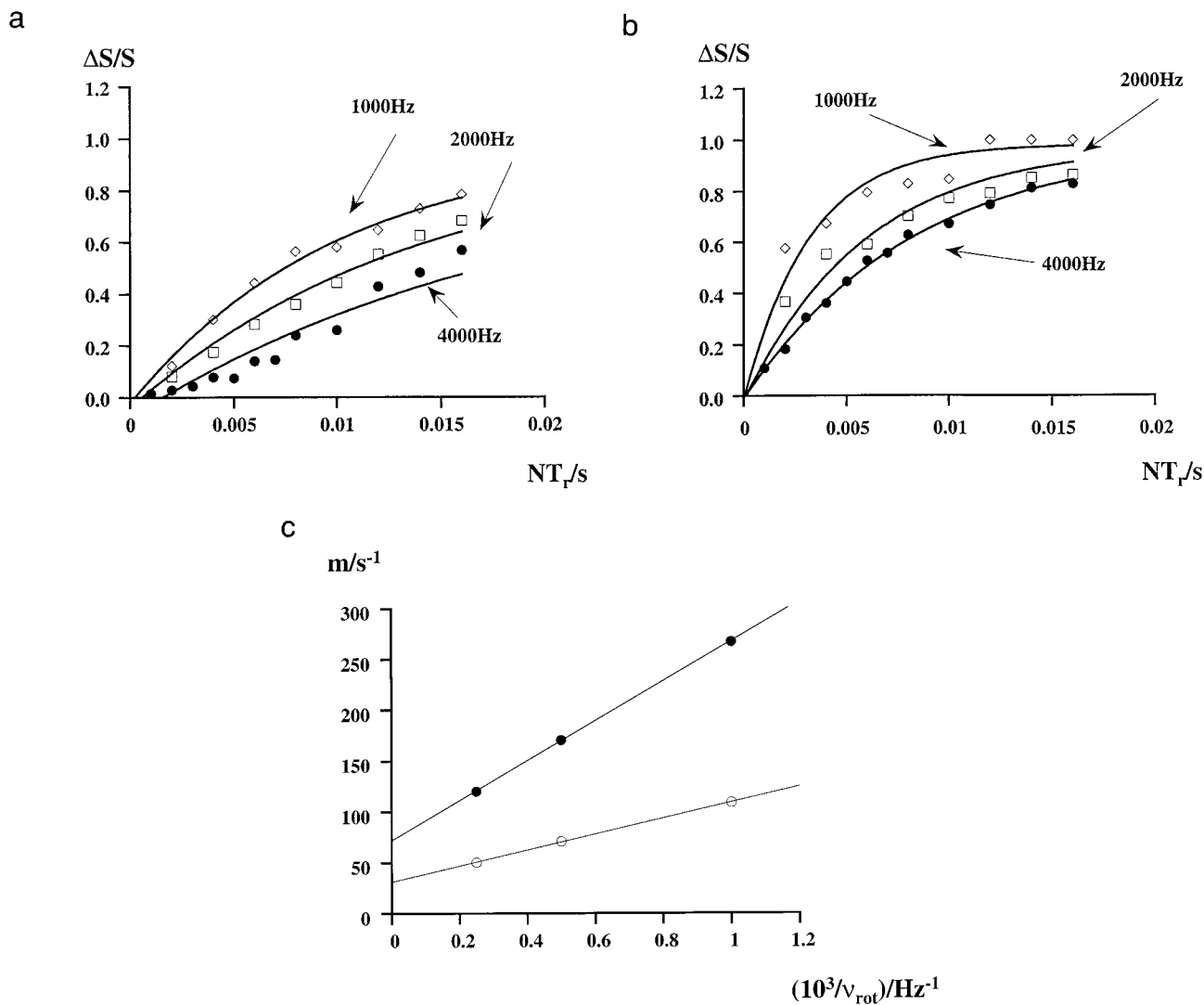


FIG. 6. (a) Plot $\Delta S/S_0$ versus dipolar evolution time for the methyl carbon (C_1) of $Al(acac)_3$ at three different MAS frequencies. (b) Plot $\Delta S/S_0$ versus dipolar evolution time for the carbonyl carbon (C_2) of $Al(acac)_3$ at three different MAS frequencies. Solid lines are fits to the function $\Delta S/S_0 = 1 - \exp(-mNT_r)$. (c) Plot m versus inverse MAS frequency for the TRAPDOR curves shown in (a) and (b). $\nu_{MAS} = 4$ kHz, $\pi/2(^{13}C) = 6.5$ μs , $\nu_{RF}(^{27}Al) = 22$ kHz. Filled circles: carbonyl carbon; open circles: methyl carbon.

TRAPDOR effect increase with decreasing rotational frequency.

In order to obtain a more quantitative measure for the magnitude of the TRAPDOR effect we fitted the curves to an exponential function $\Delta S/S_0 = 1 - \exp(-mNT_r)$. Henceforth, the parameter m defining the steepness of the curves will be used as a measure for the magnitude of the TRAPDOR effect. It is clear from inspection of Fig. 6c (plot m versus $1/\nu_{rot}$) that the magnitude of the TRAPDOR effect is inversely proportional to the MAS frequency.

The TRAPDOR results for the aluminum acetates $Al(Oac)_2OH$ and $Al(Oac)_3$ are collected in Fig. 7. The $Al(Oac)_3$ sample was further used to study the effect of the

^{27}Al RF amplitude on the magnitude of the TRAPDOR effect. To this end, the TRAPDOR curves were recorded at different ^{27}Al RF amplitudes and fitted to the function $\Delta S/S_0 = 1 - \exp(-mNT_r)$. The results for the two carbon resonances, carboxylate carbon (full circles) and methyl carbon (open circles) are plotted in Fig. 8. From inspection of this figure we find a quadratic dependence of the magnitude of the TRAPDOR effect on the ^{27}Al RF amplitude.

Finally, Fig. 9 shows the results of the TRAPDOR studies on $Al(lact)_3$. For this compound (and for $Al(acac)_3$) the crystal structure is known, allowing comparison of the TRAPDOR results with the crystal structure data.

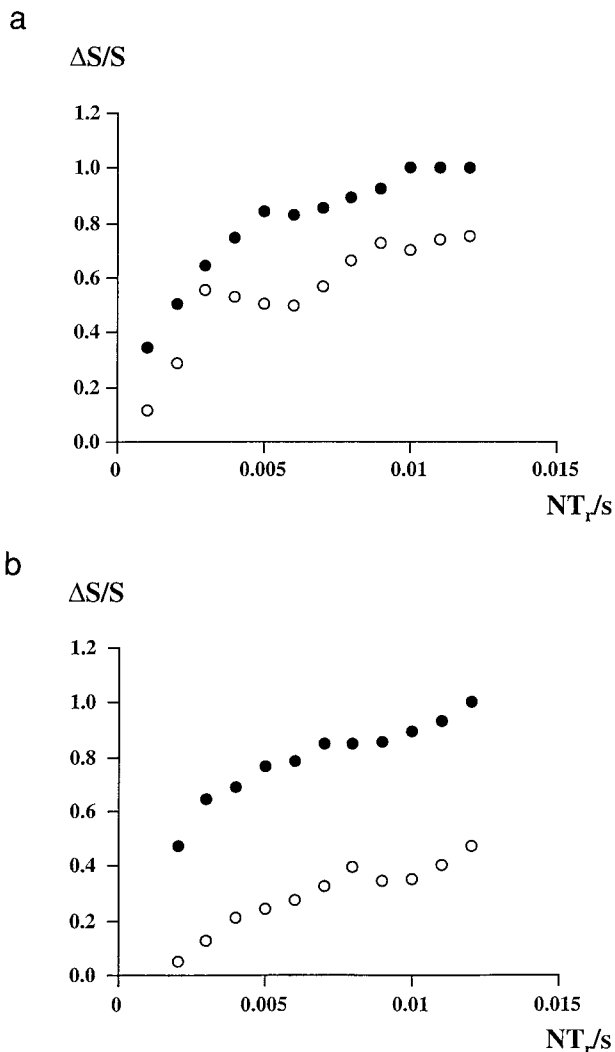


FIG. 7. Plots $\Delta S/S_0$ versus dipolar evolution time for (a) $\text{Al}(\text{Oac})_2\text{OH}$ at $\nu_{\text{MAS}} = 2$ kHz, $\pi/2(^{13}\text{C}) = 6.5$ μs , $\nu_{\text{RF}}(^{27}\text{Al}) = 17$ kHz; (b) $\text{Al}(\text{Oac})_3$ at $\nu_{\text{MAS}} = 2$ kHz, $\pi/2(^{13}\text{C}) = 7.0$ μs , $\nu_{\text{RF}}(^{27}\text{Al}) = 19$ kHz. Filled circles: carbonyl carbon; open circles: methyl carbon.

DISCUSSION

Overall Considerations

The TRAPDOR curves for the four different samples, $\text{Al}(\text{acac})_3$, $\text{Al}(\text{lact})_3$, $\text{Al}(\text{Oac})_2\text{OH}$, and $\text{Al}(\text{Oac})_3$, in Figs. 4, 7, and 9 show in all cases the highest initial slope and steepness (largest TRAPDOR effect) for the oxygen-bound carbon and the smallest for the methyl group carbon. For the samples $\text{Al}(\text{lact})_3$ and $\text{Al}(\text{acac})_3$ these findings can be related to the known crystal structures.

The asymmetric unit of the structure of $\text{Al}(\text{lact})_3$ (22) ($P2_1$, monoclinic), consists of two different monomeric $\text{Al}(\text{lact})_3$ building units; Al is coordinated by the carboxylate and hydroxyl groups of the lactate molecules in a distorted octahe-

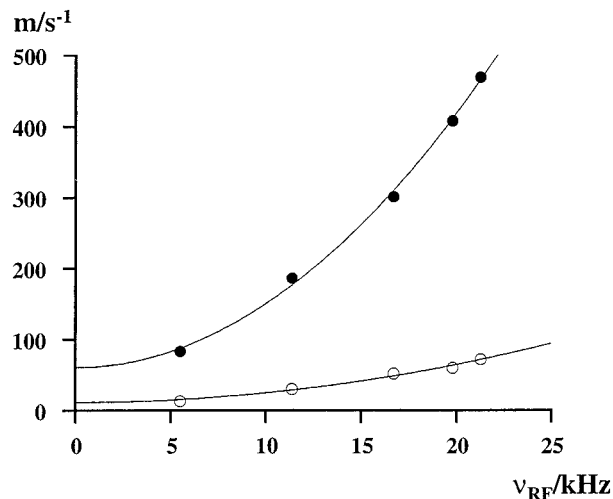


FIG. 8. m as a function of the ^{27}Al RF amplitude. Filled circles: $\text{Al}(\text{Oac})_3$ carboxylate carbon resonance; open circles: $\text{Al}(\text{Oac})_3$ methyl carbon resonance. Solid lines are guides to the eye only. $\nu_{\text{MAS}} = 2$ kHz, $\pi/2(^{13}\text{C}) = 7.0$ μs .

dron. The mean C–Al distances for the three different carbons are summarized in Table 1.

In $\text{Al}(\text{acac})_3$ (23) (monoclinic, space group $P2_1/c$) the structure consists of isolated $\text{Al}(\text{acac})_3$ molecules in which aluminum is coordinated rather symmetrically by six oxygens (from three acetylacetonate ligands). The three C–Al distances are found in Table 1. In both cases the crystal structure data are in qualitative agreement with the TRAPDOR results; the resonances for the carboxylate carbon in $\text{Al}(\text{lact})_3$ (2.7 Å) and the carbonyl carbon in $\text{Al}(\text{acac})_3$ (2.83 Å) show the largest TRAPDOR effect, followed by the C–OH carbon signal (2.85 Å, $\text{Al}(\text{lact})_3$) and the CH carbon resonance (3.2 Å, $\text{Al}(\text{acac})_3$).

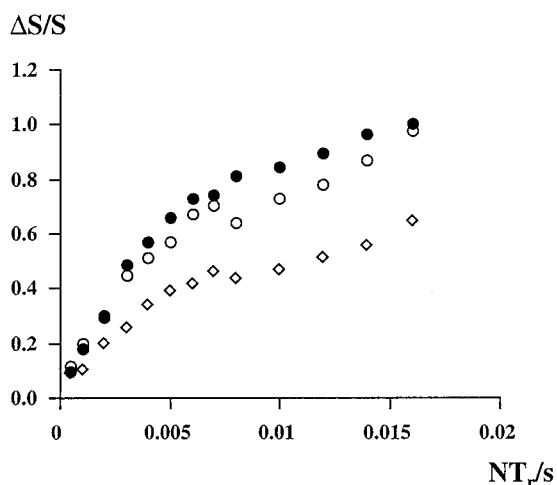


FIG. 9. Plot $\Delta S/S_0$ versus dipolar evolution time for $\text{Al}(\text{lact})_3$ at $\nu_{\text{MAS}} = 4$ kHz, $\pi/2(^{13}\text{C}) = 9.0$ μs , $\nu_{\text{RF}}(^{27}\text{Al}) = 19$ kHz. Filled circles: carboxylate carbon; open circles: C_2 -carbon; open diamonds: methyl carbon.

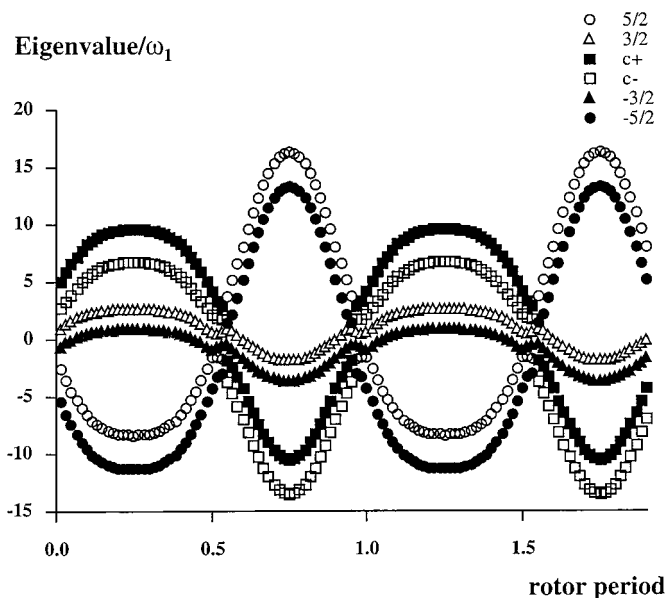


FIG. 10. Time dependence of the energy levels of the six different spin states for $I = \frac{5}{2}$ under the Hamiltonian $\mathbf{H} = \mathbf{H}_Q + \mathbf{H}_{\text{offset}} + \mathbf{H}_{\text{RF}}$ (24). $\omega_1 = 50$ kHz; $\delta = 30$ kHz; $\nu_Q = 300$ kHz. The time dependence of the quadrupolar splitting is given by $\sqrt{2} \sin 2\beta \cos(\alpha + \omega_1 t) + \sin^2 \beta \cos(2\alpha + 2\omega_1 t)$. $\alpha = \pi/2$, $\beta = \pi/6$.

Finally, the methyl carbon signals (3.9 Å, Al(lact)₃; 4.2 Å Al(acac)₃) exhibit the smallest TRAPDOR effect.

Comparison TRAPDOR/REDOR

The results in Fig. 5 indicate that the TRAPDOR approach works far more efficiently in detecting and resolving ¹³C–²⁷Al internuclear dipolar couplings than does REDOR. This result can be explained by considering the origins of the dipolar dephasing for REDOR and TRAPDOR from a quantum mechanical point of view. In the regime of moderate pulse power (selective excitation) used in this work the REDOR ²⁷Al π pulses invert (at least to a large extent) exclusively the populations of the central $|\pm \frac{1}{2}\rangle$ transition; therefore approximately one-third of the ¹³C nuclei in proximity to ²⁷Al experience dipolar dephasing, thus leading to a REDOR curve leveling off near a limiting value of $\Delta S/S_0 = 0.33$. In this simplified model, ¹³C–²⁷Al intermolecular interactions are not considered. These interactions, although with a very small dipolar coupling constant, would lead to $\Delta S/S_0$ versus NT_r curves with rather small initial slopes but nonetheless showing full dephasing ($\Delta S/S_0 = 1$) at very long dipolar evolution times.

The TRAPDOR effect relies on the fact that the energy levels for the ²⁷Al spin system under the relevant Hamiltonian $\mathbf{H} = \mathbf{H}_Q + \mathbf{H}_{\text{RF}} + \mathbf{H}_{\text{offset}}$ become time dependent under MAS. Figure 10 shows the energies of the six different spin states as a function of the rotor period. During the zero crossings transfer of populations may take place. As an example, spins orig-

inating in the $c+$ spin state ($1/\sqrt{2}$) ($|\frac{1}{2}\rangle + |-\frac{1}{2}\rangle$) (24) are transferred into the state $|\frac{5}{2}\rangle$ and vice versa.

Thus, in principle all spin states are involved in population transfers, and all ¹³C nuclei in proximity to ²⁷Al contribute to dipolar dephasing.

Controlling the TRAPDOR Efficiency

According to Vega (24), the efficiency of the population transfer can be described by an adiabaticity parameter α , defined as $\alpha = \nu_{\text{RF}}^2/\nu_Q\nu_{\text{MAS}}$. The results illustrated in Fig. 6c (linear dependence of m on $1/\nu_{\text{MAS}}$) and Fig. 8 (quadratic dependence of m on ν_{RF}^2 (²⁷Al)) reveal that the parameter m that we introduced to describe the magnitude of the TRAPDOR effect is closely related to the parameter α . Both exhibit the same dependencies on ν_{RF} , ν_Q , and ν_{MAS} ; the parameter m additionally contains the dipolar interaction strength (vide infra).

The results further disclose a procedure for maximizing the TRAPDOR efficiency. Thus, optimum TRAPDOR conditions are found at the highest possible RF amplitudes combined with relatively slow sample spinning. Of course, the proper choice of the MAS frequency involves a trade-off between spectral resolution and TRAPDOR efficiency.

Estimation of Internuclear Distances

The results presented illustrate a dependence of the magnitude of the TRAPDOR effect on the MAS frequency, the ²⁷Al RF amplitude, and the strength of the dipolar coupling of the ¹³C–²⁷Al spin pair. This opens up the possibility of manipulating the magnitude of the TRAPDOR effect and hence an optimization of the experiment, but on the other hand complicates comparison of data from different samples and experiments and extraction of ¹³C–²⁷Al distances.

Since it is the goal of these experiments to extract distance information, we must find a representation in which the influence of ν_{MAS} , ν_{RF} , and ν_Q is removed. If the magnitude of the TRAPDOR effect is plotted versus the adiabaticity parameter α for a specific ¹³C–²⁷Al dipolar interaction, then the slope of the data in this representation should be dominated by the dipolar coupling constant and hence by the ¹³C–²⁷Al internuclear distance. Figure 11 shows such a representation for the different carbon nuclei of the samples studied.

The data for the methyl groups of the Al(lact)₃ (3.9 Å), Al(acac)₃ (4.2 Å), and Al(Oac)₃ more or less show the same slope in this representation. This holds also for the data for the carboxylate carbons of Al(lact)₃ (2.7 Å) and Al(Oac)₃. With the exception of the Al(Oac)₂OH data there seems to be a qualitative correlation between the slope in an m versus α representation and internuclear distances. This approach allows a rough estimate of ¹³C–²⁷Al distances.

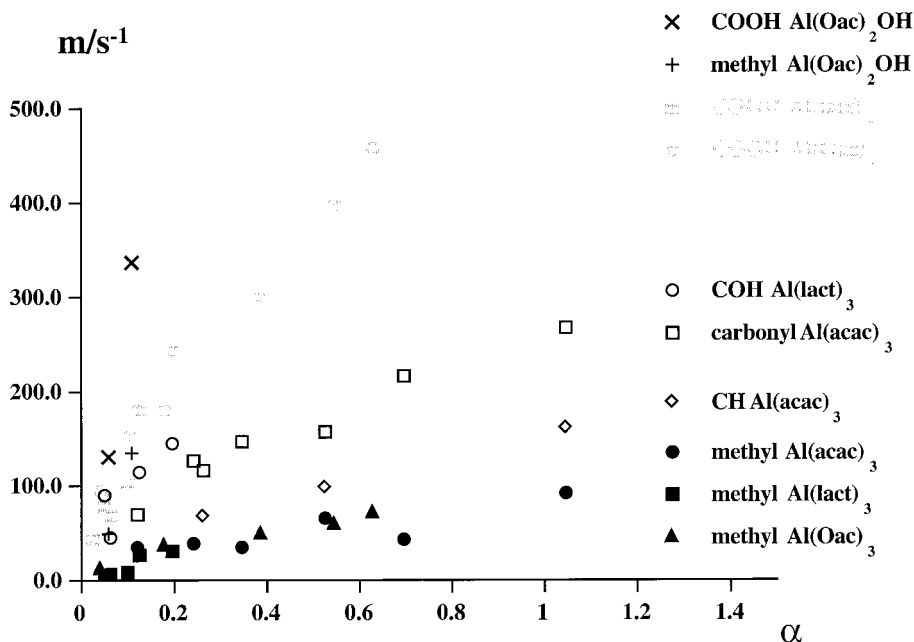


FIG. 11. Plot m versus the dimensionless adiabaticity parameter α .

SUMMARY

^{13}C - ^{27}Al dipolar couplings were detected using modified double resonance techniques. The pulses for both nuclei (^{13}C and ^{27}Al) were applied to the same probe channel. The TRAPDOR approach proves to be much more effective in resolving different dipolar coupling strengths than REDOR. TRAPDOR offers opportunities to tune the experiment to high sensitivity by adjusting the rotational frequency and ^{27}Al RF amplitudes. Where known, the crystal structure data are in qualitative agreement with the results extracted from our experiments. The presented dependence of the magnitude of the TRAPDOR effect on the adiabaticity parameter α is a promising approach to the goal of extracting quantitative distance information.

REFERENCES

1. E. R. H. van Eck, R. Janssen, W. E. J. R. Maas, and W. S. Veeman, *Chem. Phys. Lett.* **174**, 428 (1990).
2. C. P. Grey and W. S. Veeman, *Chem. Phys. Lett.* **192**, 379 (1992).
3. C. P. Grey, W. S. Veeman, and A. J. Vega, *J. Chem. Phys.* **98**, 7711 (1993).
4. C. P. Grey, A. P. A. M. Eijkelenboom, and W. S. Veeman, *Solid State NMR* **4**, 113 (1995).
5. T. Gullion and J. Schaefer, *J. Magn. Reson.* **81**, 196 (1989).
6. Y. Pan, T. Gullion, and J. Schaefer, *J. Magn. Reson.* **90**, 330 (1990).
7. A. Naito, K. Nishimura, S. Tuzi, and H. Saito, *Chem. Phys. Lett.* **229**, 506 (1994).
8. T. Gullion, *J. Magn. Reson.* **117**, 326 (1995).
9. L. Chopin, S. Vega, and T. Gullion, *J. Am. Chem. Soc.* **120**, 4406 (1998).
10. E. R. H. van Eck and W. S. Veeman, *J. Am. Chem. Soc.* **115**, 1168 (1993).
11. H. M. Kao and C. P. Grey, *J. Phys. Chem.* **100**, 5105 (1996).
12. C. A. Fyfe, K. C. Wong-Moon, Y. Huang, H. Grondy, and K. T. Mueller, *J. Phys. Chem.* **99**, 8707 (1995).
13. C. P. Grey and A. J. Vega, *J. Am. Chem. Soc.* **117**, 8232 (1995).
14. C. P. Grey and B. S. A. Kumar, *J. Am. Chem. Soc.* **117**, 9071 (1995).
15. C. A. Fyfe, K. T. Mueller, H. Grondy, and K. C. Wong-Moon, *Chem. Phys. Lett.* **199**, 198 (1992).
16. L. van Wüllen, L. Züchner, W. Müller-Warmuth, and H. Eckert, *Solid State NMR* **6**, 203 (1996).
17. K. Herzog, B. Thomas, D. Sprenger, and C. Jäger, *J. Non-Cryst. Solids* **190**, 296 (1995).
18. A. L. Blumenfeld, D. J. Coster, and J. J. Fripiat, *Chem. Phys. Lett.* **231**, 491 (1994).
19. L. van Wüllen, *Solid State NMR* **13**, 123 (1998).
20. C. Jäger, W. Müller-Warmuth, C. Mundus, and L. van Wüllen, *J. Non-cryst. Solids* **149**, 209 (1992).
21. N. C. Nielsen, H. Bildsoe, H. J. Jacobsen, and J. Skibsted, *J. Magn. Reson.* **95**, 88 (1991).
22. G. G. Bombi, B. Corain, A. A. Sheik Osman, and G. C. Valle, *Inorg. Chim. Acta* **171**, 79 (1990).
23. P. K. Hon and C. E. Pflugler, *J. Coord. Chem.* **3**, 67 (1973).
24. A. J. Vega, *J. Magn. Reson.* **96**, 50 (1992).